

Unraveling the relationship between geomorphodiversity and sediment connectivity in a small alpine catchment

Irene Maria Bollati¹  | Marco Cavalli² 

¹Earth Science Department "Ardito Desio", Università degli Studi di Milano, Milan, Italy

²Research Institute for Geo-Hydrological Protection, Padua, Italy

Correspondence

Irene Maria Bollati, Earth Science Department "Ardito Desio", Università degli Studi di Milano, Milan, Italy.
Email: irene.bollati@unimi.it

Abstract

Mountain regions are characterized by a spatial geomorphic heterogeneity that confers on the environment a significant geomorphodiversity. A methodology based on a different scale/spatial/resolution approach is proposed to evaluate the relationship existing among geomorphodiversity, geomorphological processes, and sediment connectivity. Starting from the geomorphological mapping of the Veglia Devero Natural Park (Lepontine Alps), indexes of fragmentation (*IFrm*) and geomorphodiversity (*IGmf*) were computed. The results were used to select a meaningful sub-area (Buscagna stream catchment) for calculating the index of connectivity (*IC*). The relationships among these three indexes are discussed, using a semi-quantitative approach including descriptive statistics (i.e., box plot) and analysis of the different *geomorphoconnectivity sectors*, testifying to the role of geomorphic processes in regulating sediment fluxes and, consequently, controlling landscape units. *IGmf* turned out to be more conservative than *IFrm* and more management-oriented for protected areas, while *IC* was confirmed to be particularly suitable to characterize connectivity in small mountain catchments featuring different geomorphic processes and a complex topography. This study suggests that coupling the sediment connectivity with the geomorphology and geomorphodiversity of a given area

This is an open access article under the terms of the Creative Commons Attribution License, which permits use, distribution and reproduction in any medium, provided the original work is properly cited.

© 2021 The Authors. *Transactions in GIS* published by John Wiley & Sons Ltd.

represents a quite novel approach that could be usefully applied in the framework of protected areas to investigate also biodiversity patterns and consequently environmental evolution in space and time.

1 | INTRODUCTION

Geomorphic systems may exhibit extremely variable behavior over short distances, especially in mountain environments where *geodiversity* is considered particularly relevant (Bollati et al., 2016; Brocx & Semeniuk, 2007; Gordon, 2018; Zwoliński, 2009). Several definitions of geodiversity have been proposed in the literature, considering mainly geological (rocks, minerals, fossils), geomorphological (landform, processes) and soil features (Dixon, 1996; Gray, 2004). The interest in geodiversity has been growing since the 1990s, with several years characterized by a peak in scientific production (Bollati, Paleari, Zanoletti, & Pelfini, 2017). Moreover, considering the richness and variety of geomorphological elements in an area, *geomorphodiversity* is an important concept, defined as “geodiversity with respect to geomorphology” (sensu Panizza, 2009).

Qualitative evaluations of geodiversity, in general, rely on the categorization of values and ecosystem services as proposed by Gray, Gordon, and Brown (2013), who ascribed to geodiversity the regulation, support, provisioning, and cultural functions. The authors, along with others (Gordon, 2018; Washington, 2018), stress the meaning of geodiversity within the framework of biodiversity but, at the same time, also stress its independent and intrinsic value. As for biodiversity, the need for the quantification of this feature soon emerged and methodological approaches were gradually developed to address this issue. In particular, according to Bollati et al. (2016, and references therein), the quantification of geodiversity can be approached at three levels: (a) at the level of a single site (*site intrinsic geodiversity*); (b) within a region (*regional intrinsic geodiversity*); (c) at the regional level in comparison with other regions (*extrinsic geodiversity*).

Level (b) is the one most frequently adopted since it can be easily implemented for management purposes in specific areas. For its computation, several methods are proposed (see the review in Zwoliński, Najwer, & Giardino, 2018), and two main categories of quantification methods exist, as suggested by Pellitero, Manosso, and Serrano (2015).

Direct methods (e.g., Carcavilla, López-Martínez, & Durán, 2007; Pereira, Pereira, Brilha, & Santos, 2013) are aimed at counting and summing up features belonging to different families to determine the *richness of certain categories of elements of an area* (e.g., geology, geomorphology, paleontology, mineralogy). In a fluvial context, a similar approach was used by Singh and Sinha (2020) to analyze the distribution and diversity of the floodplain wetlands. The method usually starts with pre-elaborated thematic maps (geological, geomorphological, soil, or resource maps) used as input data for further GIS elaborations. The study areas are generally subdivided into cells of different size depending on the width of the whole area and on the purpose of the analysis. These methods require a pre-processing step, mainly aimed at homogenizing data from different sources. Subjectivity, possibly due to the interpretative nature of the input data, should be also taken into account in the final result (Melelli, Vergari, Liucci, & Del Monte, 2017).

Indirect methods (e.g., Melelli et al., 2017; Zwoliński, 2009) imply the use of geomorphometry since they are based on the use of a digital elevation model (DEM) and its derivatives, to compute physical properties of the terrain (e.g., surface roughness), whose variability can be interpreted as the geomorphodiversity of the area. In this case, input data have a higher degree of objectivity with respect to the previous approach since they are mainly independent of any interpretation by the operator (except in the case of the choice of the computational approaches and related parameters). In conclusion, indirect methods retrieve relief diversity from automatic procedures on DEMs, considering morphometric and hydrological properties. Besides the issue of subjectivity related to the use of geomorphological maps

as input data, indirect methods could be preferred due to the lack of geomorphological maps, elaborated with homogeneous criteria, that cover different territories (Melelli et al., 2017).

Since the scope of the present research is the comparison of the geomorphodiversity index with a morphometry-based one, the importance of disentangling landform convergence (e.g., a scarp could be originated by different processes) turns out to be fundamental. Unfortunately, indirect methods lack information on genetic processes of physical relief, even if in some cases the geomorphological map has been used as a comparison after the computation of the morphometry-based index (i.e., indirect method; Melelli et al., 2017).

The linkage between different areas of a catchment expressed through the erosion–transport–sedimentation patterns along channel networks and on the hillslopes, surely plays a relevant role in geomorphodiversity analyses. Besides the various mentioned aspects, geomorphodiversity is also strictly related to the dynamic behavior of geomorphic systems that is strongly connected to topographic features variability. Especially in mountain areas, sediment fluxes are controlled by intrinsic properties such as topography, landforms, land use, and by external drivers such as precipitation and snow/glacier meltwater discharge. Also, geomorphic processes play a relevant role along with human impact that heavily affects landscape (Heckmann et al., 2018). All these aspects are related to the concept of *sediment connectivity*, which can be defined as the degree of linkage (lateral, longitudinal, and vertical) that controls sediment fluxes throughout the landscape (Cavalli, Trevisani, Comiti, & Marchi, 2013). Sediment connectivity represents an emerging property of a geomorphic system (i.e., coupling relationship between elementary units: landforms, slope units, sub-catchments) and reflects the potential of water/sediment to move through the system (Cavalli, Heckmann, & Marchi, 2019; Heckmann et al., 2018; Singh et al., 2021). Sediment connectivity is pivotal for the geomorphic understanding of a landscape. Indeed, the analysis of landscape structure, that is, the spatial configuration of landforms, along with an understanding of the relationships linking landscape compartments, helps throw light on the role of geomorphic processes in a catchment (Brierley, Fryirs, & Jain, 2006; Harvey, 2001; Hooke, 2003). In particular, it has been demonstrated how (dis)connectivity controlled by the positioning of landforms acting as blockages with respect to sediment fluxes in a catchment may affect sediment delivery (Fryirs, 2013; Fryirs, Brierley, Preston, & Kasai, 2007). According to several authors (e.g., Cavalli, Vericat, & Pereira, 2019; Heckmann et al., 2018; Wainwright et al., 2011), it is possible also to distinguish between *structural connectivity* that describes the spatial contiguity of landscape units and *functional connectivity* that is process-based. In this last case, considering geomorphic systems and the related sediment connectivity (Messenzehl, Hoffmann, & Dikau, 2014) as a functional component of ecosystems, the influence on soil development, and consequently on vegetation, could be highly relevant (Seijmonsbergen, Van den Ancker, Jungerius, & Norder, 2019). Vegetation, in fact, could interfere with geomorphic dynamics, being a regulating agent, but also suffering from the impact of geomorphic processes (Bollati, Crosa Lenz et al., 2018; Germain, Gavrilă, Elizbalashvili, & Pop, 2020; Savi, Schnewly-Bollschiweiler, Bommer-Denns, Stoffel, & Schlunegger, 2013).

The main aim of this work is hence the assessment, through specific indexes, of the relationship existing among geomorphological systems, sediment connectivity, and geomorphodiversity. The analysis of the relation between geomorphodiversity and sediment connectivity represents a quite novel topic. To this end, geomorphodiversity indexing was primarily focused, at a wider scale, on the Veglia Devero Natural Park (VDNP, Lepontine Alps) through the application of a direct method calculating the richness of geomorphological elements of the study area. Geomorphological maps, used as input data, are indeed a good means of landscape analysis, including information on the geology of the bedrock (including lithology and structure), morphography, morphometry, morphodynamics and morphochronology, classifying the elements according to their genetic processes (i.e., morphogenetic approach) (Bollati, Cerrato, et al., 2018; Campobasso et al., 2018; Castiglioni, 1966; Rădoane, Cristea, & Rădoane, 2011; Verstappen, 2011). The main aim of this analysis is the investigation of the relationship between geomorphological features and their variety with respect to sediment connectivity. As depicted in several examples in the literature, geomorphological maps represent valuable input data to develop sediment storage maps in view of sediment connectivity analyses (e.g., Buter, Spitzer, Comiti, & Heckmann, 2020; Otto, Schrott, Jaboyedoff, & Dikau, 2009; Theler, Reynard, Lambiel, & Bardou, 2010).

To this end and in order to avoid redundancy, a direct method has been preferred since it uses as input data a geomorphological map including the genesis of the relief, not only their morphometric properties, which are already considered in the geomorphometric sediment connectivity indexing computation. Hence, based on the results obtained from indexing the geomorphodiversity of VDNP territory, the Buscagna stream catchment (12 km²) was then selected for a sediment connectivity evaluation at a finer spatial scale, to compare the results with geomorphodiversity data. This sub-catchment was selected since it is characterized by a dichotomy between the two valley slopes, mainly concerning lithological differentiation and related surface processes. This feature allows the area to be used as a test-site for different scientific purposes (e.g., Masseroli, Bollati, Proverbio, Pelfini, & Trombino, 2020), as the geomorphodiversity-connectivity comparison, herein explored.

2 | STUDY AREA

The VDNP is located in the Lepontine Alps, on the border between Italy and Switzerland, and it partially overlaps with the Special Protection Area named “Alpi Veglia e Devero—Monte Giove” (151.19 km²). The area is located in the Alpine chain, and in particular in the Ossola-Simplon belt, the Europe-verging portion of the Alpine chain. The upper and lower Penninic Domains, representing the deepest portion of the Alpine chain, outcropping due to the uplift by the Simplon Line during the Oligocene-Miocene, characterize the study area (e.g., Bigioggero, Colombo, Cavallo, Aldighieri, & Tunesi, 2007; Steck, 2008). These structural domains include metamorphic rocks deriving from the transformation of an ancient basement and the relatively heterogeneous metasedimentary coverage (Bigioggero et al., 2007). In general, gneiss (Monte Rosa unit, Monte Leone, Pioda di Crana, and Antigorio nappes), metaconglomerate (Lebendun nappe), and calcschist (Valais calcschist units) are structurally alternating. Locally, ultramafic rocks outcrop (Cervandone-Geisspfad unit).

Within the VDNP, the Buscagna stream catchment was selected for the more detailed analyses. It runs SW-NE and ranges in altitude from 1,650 m a.s.l. (Devero plain) to 3,237 m a.s.l. (Boccareccio Peak). The Buscagna valley is a glaciostructural valley set along the contact between gneisses (Monte Leone Unit), and calcschist with marbles (Valais Unit), where rocky outcrops were intensely shaped by glaciers. In the catchment, ultramafic rocks, mainly serpentinite (Ultramafic Cervandone-Geisspfad Complex within Monte Leone unit), and metaconglomerate and paragneiss (Lebendun and Berisal units) locally outcrop. The geomorphologically dominant features mirror both lithological and structural settings of the catchment (Masseroli et al., 2020). Gneisses, prevailing along the NW slope characterized by a high relief energy (e.g., Boccareccio Peak, 3,237 m a.s.l.; B in Figure 1), are competent, affected by cryoclastism and gravity-related processes such as rockfall and debris flow. Along the northern foot-slope, composite cones (*sensu* Baroni, Gentili, & Armiraglio, 2013), fed by different processes (water-related, mass wasting and snow avalanches), are recurrent elements (Figure 1).

Carbonatic rocks outcrop along the SE side of the catchment (e.g., Cazzola Mount, 2,330 m a.s.l.; A in Figure 1). Calcschist and marble are more suitable for chemical dissolution and erosion, and are affected by hypogean and epigean karst processes generating typical landforms: caves, sinkholes, enlarged fractures, following a double-oriented regional trend (E-W and NNE-SSW), trenches and a V-shaped small valley. Moreover, due to the dip-slope dipping schistosity, towards NW, rock-slides occur on this side of the valley.

The structural contact between Monte Leone and Valais units, running along the valley bottom, near the NW foot-slope, is covered by Quaternary deposits of different genesis (glacial, gravity-, snow-, and water-related).

Landforms derived from glacial, periglacial, and paraglacial dynamics are very widespread. Pleistocene glacial activity left recurrent signs in the landscape (Sacco, 1930): abundant glacial debris (e.g., moraines and erratics), transversal and lateral glacial steps, hanging glacial valley and basins. In these lateral hanging glacial basins Holocene glaciers were present. Currently, due to the morphometry and topographic features of the basin, glaciers are practically extinct (Diolaiuti & Smiraglia, 2015). On the calcschist side, the glacial modeling is very relevant and on the top of the slopes glacial deposits locally cover the surface eroded by the glacier.

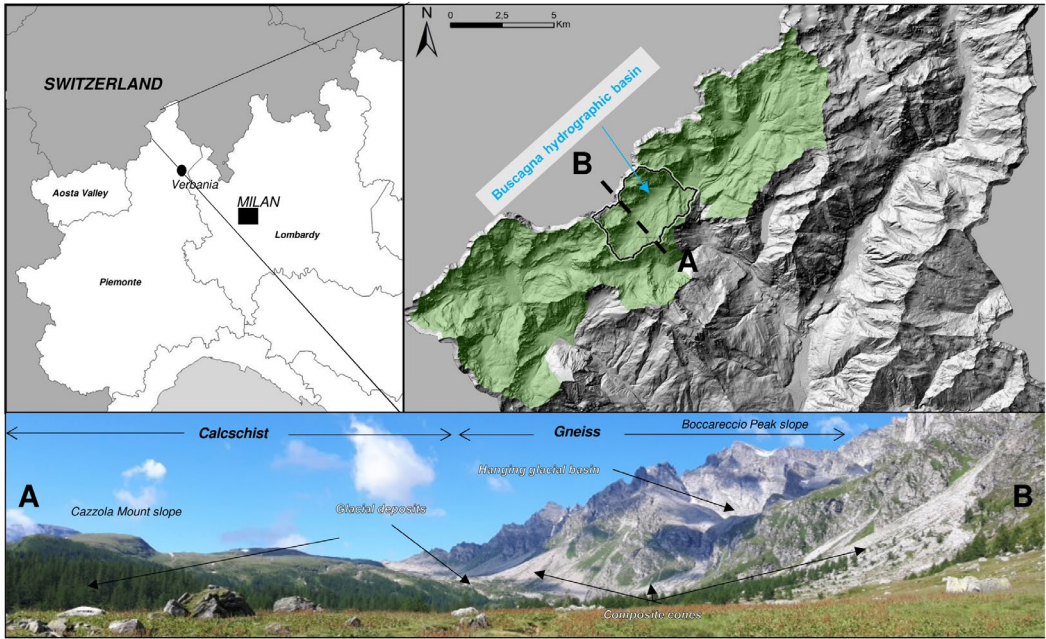


FIGURE 1 Overview of the study area and its location in northwest Italy. The green area, covered by the geomorphological mapping and geomorphodiversity indexing, includes the protected area of the VDP with the SIC (SCI-Site of Community Importance) and ZPS (Special Protection Area [SPA]) area. The black-bordered area is the Buscagna hydrographic basin on which sediment connectivity analyses are conducted

At higher altitudes, deposits related to glacial activity (moraines) have been undergoing reworking by paraglacial-type dynamics (sensu Ballantyne, 2002).

Snow avalanches, feeding composite cones, on some occasions dammed the Buscagna stream. This happened, for example, during the event that occurred in spring 2018 (Masseroli et al., 2020). Block fields and hypothetical rock glaciers are also present, where morphological signs have been detected, coinciding with the possible presence of permafrost according to the model proposed by Boeckli, Brenning, Gruber, and Noetzli (2012).

The Buscagna stream drains the valley bottom and it assumes a meandering pattern upstream with respect to the Pleistocene moraines. Here a peatbog of high naturalistic value is present.

Soil dynamics reflect this geomorphic dichotomy, testifying to past and present erosion and deposition stages (Masseroli et al., 2020).

3 | METHODS

3.1 | Calculation of the index of geomorphodiversity and index of fragmentation

In this subsection the procedure for the calculation of the *index of geomorphodiversity* and *index of fragmentation* is described.

3.1.1 | Cell size choice

Geomorphodiversity indexing requires a preliminary determination of the cell size, here decided according to:

1. the extent of the area (117 km²). In this sense, a literature analysis to detect similar analyses conducted in areas with similar extent and analogous morphogenetic and morphoclimatic features was performed. Among the references retrieved, Hjort and Luoto (2010) (e.g., 285 km²) and Hjort et al. (2012) (e.g., 110 km²), working on similar-sized areas and analogous morphogenesis, were considered the most appropriate for comparison.
2. the average width of landforms polygons characterizing the area (about 77,000 m²).

For the study area, five cell sizes were then tested on a sample area of 4 km²: 100 × 100 m; 200 × 200 m, 500 × 500 m and 1,000 × 1,000 m, and 2,000 × 2,000 m. The indexes were calculated for these sample cells and the difference between the maximum and the minimum values obtained for each sample cell size for the fragmentation and geomorphodiversity indexes was considered. According to Pereira et al. (2013), this analysis could help in detecting which size of cell could maximize the differentiation and enhance feature diversity inside each cell. In Figure 2 the results of the comparison between cell sizes are reported with the calculated difference between the maximum and the minimum values of the indexes in the sample cells. For the 2,000 × 2,000 m cell size, the spatial resolution of the data was not sufficient to obtain reliable values. Moreover, for values greater than 500 × 500 (i.e., 1,000 × 1,000) the steepness of the curve indicating the divergence between the maximum and the minimum values rapidly diminishes (Figure 2). Accordingly, the best cell size value detected is 500 × 500 m (0.25 km²), which represents a good compromise between the need to maximize the diversity within the cell and to avoid dealing with too coarse resolutions. It should be noted that the other two categories tested (100 × 100 and 200 × 200 m) are below the average width of the landform size featuring the study area (77,000 m²), whereas the chosen cell size is three times this value, allowing a good maximization of diversity within the investigate area.

3.1.2 | Geomorphodiversity index calculation

The VDNP geomorphological map and the related database represent the input data for the creation of a geomorphodiversity thematic map of the VDNP. The geomorphological map was developed from the integration and digitalization of existing maps available from different sources, including the Municipality Regulating Plan, the shapefiles available from the Geoportale Regione Piemonte (<https://www.geoportale.piemonte.it/>), the

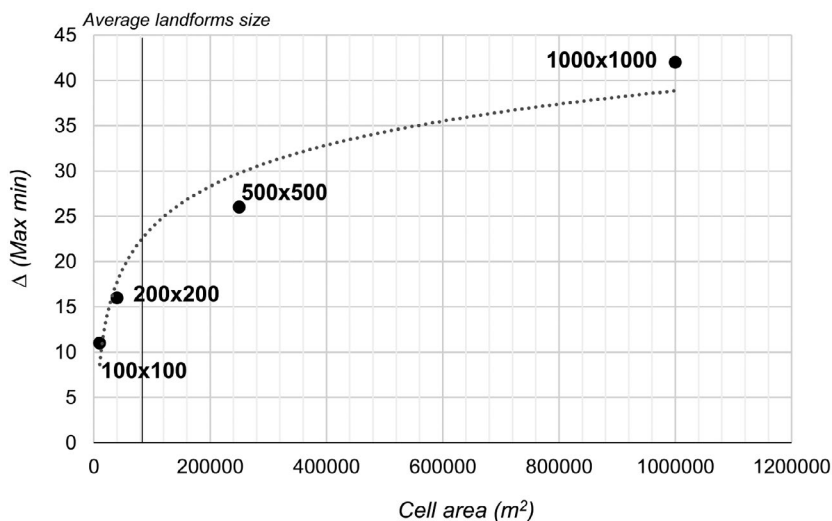


FIGURE 2 Cell size comparison for the selection of the most suitable dimension for *IFrm* and *IGmf* calculation, as a function of the average size of landforms

Geoportale Nazionale (<http://www.pcn.minambiente.it/mattm/>) and the IDROGeo Platform (<https://idrogeo.ispraambiente.it/app/>), as well as literature sources (e.g., Rigamonti & Uggeri, 2016). The classification of landforms follows the rules suggested by Campobasso et al. (2018): (i) lithologies are grouped according to their response to geomorphic processes (e.g., massive metamorphic and magmatic, schists, carbonatic rocks); and (ii) landforms are classified according to their genetic processes (e.g., gravity-related in red, water-related in green). This approach is aligned with other methods proposed by the international scientific community (e.g., Rădoane et al., 2011; Verstappen, 2011). Geomorphological mapping strategies can, moreover, vary according to specific morphogenetic environments, especially concerning specific applied issues—for example, periglacial (Gentizon et al., 2000), fluvial (Fryirs & Brierley, 2018; Wheaton et al., 2015) or glacial (Chandler et al., 2018). In the VDNP a variety of processes contribute to landscape generation (see the online Supporting Information), and landforms were hence classified according to the type of geomorphic process they were generated by: water-related, gravity-related, glacial, and periglacial processes. Moreover, karst-related landforms were mapped where soluble rocks outcrop.

The digital version of the map reproduced at a scale of 1:35,000 (online Supporting Information) consists of three different types of vector data (polygons, lines, and points according to the scale of the map and the landform size), used to design landforms belonging to the different morphogenetic categories (depicted with different colors).

Concerning geomorphodiversity indexing, two indexes, with a total of six subindexes related to polygons, lines, and points, were initially chosen and applied as a result of a review of the literature mainly focused on indexes of richness (e.g., Carcavilla et al., 2007; Pereira et al., 2013). ArcGIS 10.2 was used to compute the indexes and the complete workflow in the GIS environment is reported in Figure 3. The indexes were derived as follows:

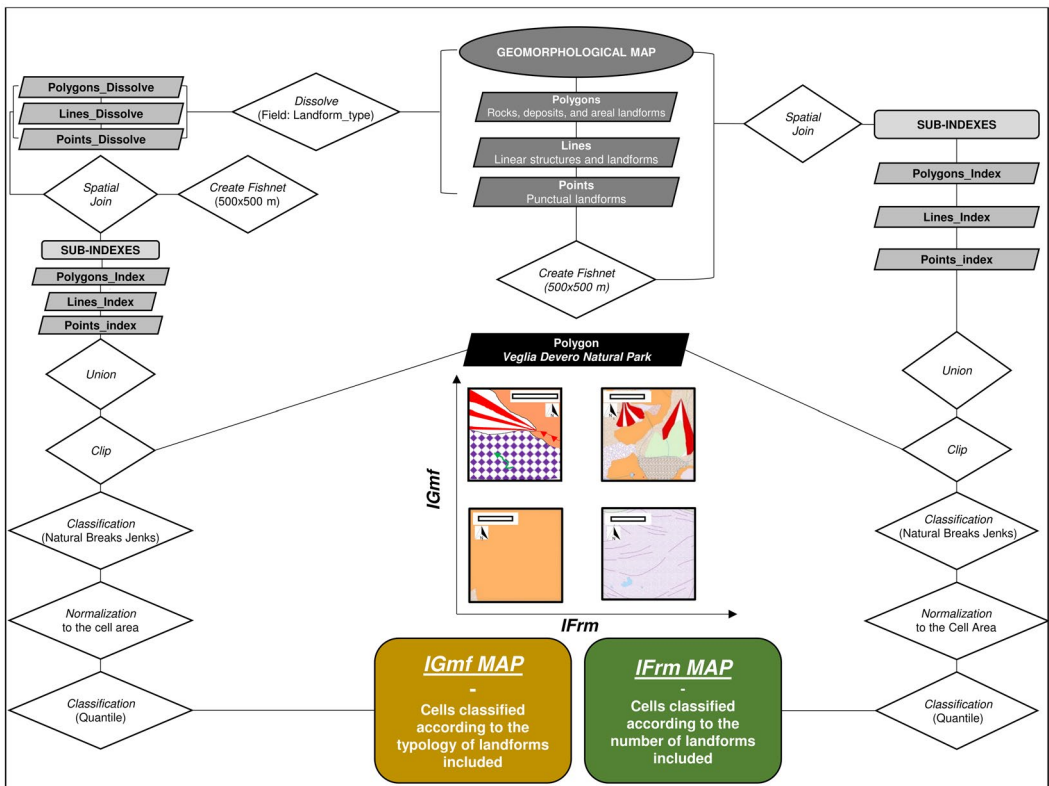


FIGURE 3 Workflow for the generation of the *IFrm* and *IGmf* thematic maps, with examples of contents in classified cells. The spatial scale on the sample cells corresponds to 200 m

- *Index of fragmentation (IFrm)*. This was calculated for each cell of the grid by summing each landform within the same cell. The final result corresponds to the number of polygons, polylines, and points contained in each cell for which *sub-IFrms* (i.e., low-order *IFrms* related to polygons, polylines, and points, to be summed to obtain the final map) were created during the procedure.
- *Index of geomorphodiversity (IGmf)*. This was calculated for each cell of the grid by summing the landforms within the same cell and then aggregated according to their typology. The operation aimed to obtain one recurrence for each type of landform in each cell. What makes the difference between cells is the number of landform types included therein. The final result corresponds to the number of polygons, polylines, and points of each cell for which *sub-IGmfs* (i.e., low-order *IGmf* related to polygon, polyline, and points, to be summed to obtain the final map) were created during the procedure.

The area of index calculation was clipped to the natural park borders. According to this approach, at the map borders some cells have a smaller area with respect to the others, potentially affecting index calculation. For this reason, the *IFrm* and *IGmf* values obtained were normalized by dividing by the area of each cell. After that, a check between the non-normalized values and the normalized values was carried out by the operator.

Finally, both *IFrm* and *IGmf* maps were elaborated by using a quantile classification method (Figure 3).

3.2 | Connectivity index calculation

The sediment index of connectivity (*IC*), proposed by Cavalli et al. (2013), is a topographic-based geomorphometric approach and it is mainly intended to assess lateral connectivity (i.e., hillslope to channel connectivity). It is given by:

$$IC = \log_{10} \left(\frac{D_{up}}{D_{dn}} \right) \tag{1}$$

where D_{up} is the upslope component expressing the potential for downward routing of the sediment produced upslope, and D_{dn} is the downslope component taking into account the flow path length that a particle has to travel to reach the nearest chosen target. D_{up} is given by:

$$D_{up} = \overline{WS} \sqrt{A} \tag{2}$$

where \overline{W} is the average weighting factor of the upslope contributing area, \overline{S} is the average slope gradient of the upslope contributing area (m/m), and A is the upslope contributing area (m²); and D_{dn} is given by:

$$D_{dn} = \sum_i \frac{d_i}{W_i S_i} \tag{3}$$

where d_i is the length of the flow path along the cell in the steepest downslope direction (m), and W and S are the weighting factor and the slope gradient of the cell, respectively. *IC* is defined on the entire real line, $[-\infty, +\infty]$, with connectivity increasing for larger *IC* values.

The weighting factor W in Equations 2 and 3 is intended to represent the impedance to sediment fluxes and can be expressed in different ways as, for example, with the C-Factor in the original version by Borselli, Cassi, and Torri (2008). In this work, as suggested in Cavalli et al. (2013), we used the geomorphometric approach based on *surface roughness* for W . Surface roughness is calculated according to Cavalli and Marchi (2008) as the standard deviation of the residual topography within a moving window. In order to perform this analysis, a high-resolution

Digital Terrain Model (DTM) is required (Cavalli & Marchi, 2008; Cavalli, Vericat, et al., 2019). The DTM used for this research is a LiDAR-based DTM with a 5 m resolution (source Geoportale Regione Piemonte; <https://www.geoportale.piemonte.it/cms/servizi/servizi-di-ricerca/5-catalogo-dei-metadati>). Considering DTM resolution, the moving window size for roughness calculation was set to 3 × 3 cells. IC computation was carried out by using SedInConnect (Crema & Cavalli, 2018), freely available at https://github.com/HydrogeomorphologyTools/SedInConnect_2.3.

The input DTM was hydrologically corrected using the Pit Remove tool of *TauDEM 5.3.7* (<http://www.engineering.usu.edu/dtarb/taudem>), whereas the catchment and the channel network were defined using the Watershed delineator of *ArcSwat 2012.10_2_19* (<https://swat.tamu.edu/software/arcswat/>).

4 | RESULTS

4.1 | Geomorphodiversity index map

The thematic maps elaborated for the *IFrm* and *IGmf* indexes cover an area of 117 km² (i.e., 562 cells). In general, the VDNP is characterized by a variable geomorphodiversity, with local hot spots, and other areas characterized by diffuse low geodiversity. For more detail, see Figure 4.

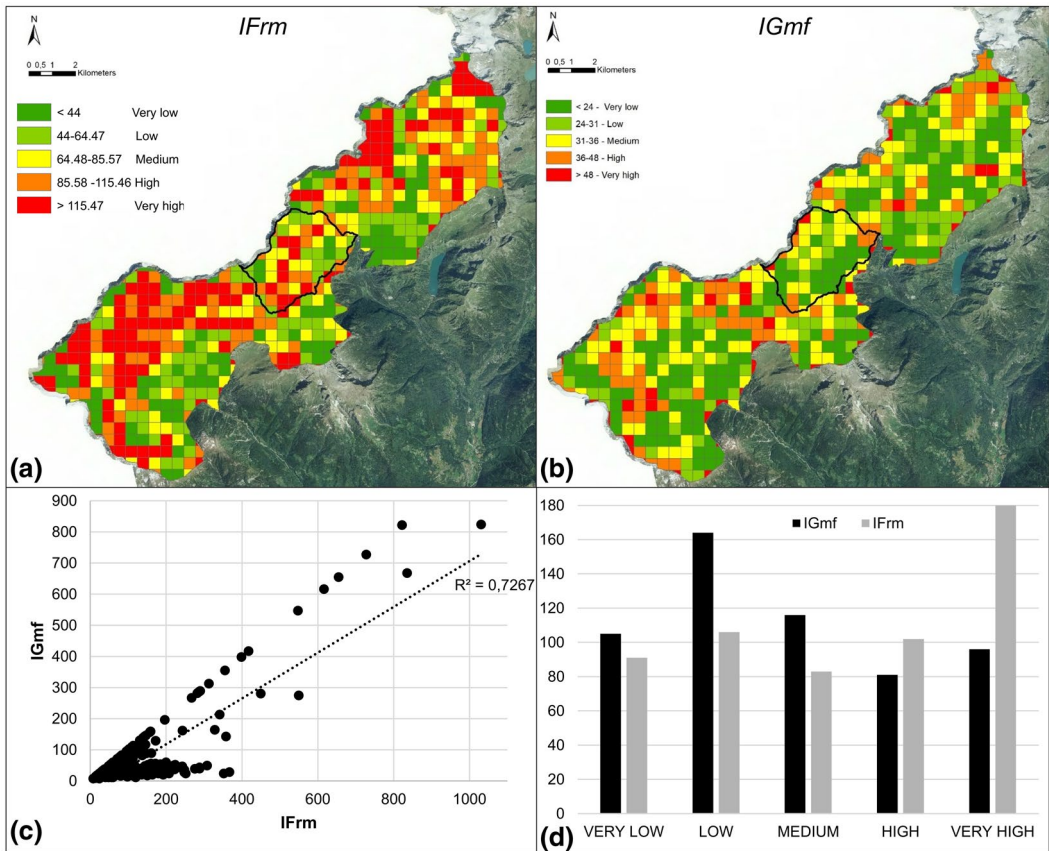


FIGURE 4 (a) *IFrm* and (b) *IGmf* thematic maps plotted over the orthophoto (rectified aerial photo) 2010 (courtesy of Geoportale Regione Piemonte). (c) The correlation between *IGmf* and *IFrm* values is relatively high, but (d) the distribution between classes is different between the indexes

Although the spatial distribution of *IFrm* and *IGmf* values appears random, a significant correlation between their values is obtained ($r = 0.7267$; Figure 4c). In general high and very high *IFrm* values (orange and red in Figure 4a) characterize about the 50% of the cells, which include several polyline- (e.g., moraine ridges or fluvial erosion scarps), or point-type elements (e.g., erratic boulders). The *IGmf* values are high and very high (orange and red in Figure 4b) for 31.5% of the cells, where geomorphic processes and related landforms are of a different type, despite the number of elements included. The percentage of cells characterized by medium to low *IGmf* is higher (69%). Of course, the linear correlation between the two indexes is influenced by the fact that the greater is the number of elements in a cell, the higher is the possibility they are related to different genetic processes (i.e., different agents, or different modes such as erosion or deposition).

Focusing on the Buscagna Stream catchment (black border in Figure 4), where the connectivity index has been also calculated, the *IFrm* map shows a random distribution of values (Figure 4a), with a predominance of medium to high values. The *IGmf* seems to have a more obvious spatial trend (Figure 4b), according to the glaciostructural valley elongation. As mentioned before, the two valley sides are clearly asymmetric due to the different susceptibilities of gneiss and calcschist to geomorphic processes, exaggerated by the regional dipping of the surfaces. The two sides are thus characterized by different types of processes, which on the northern side are even more intrinsically variable than on the southern side. On the *IGmf* map it is possible to detect a prevalence of low geomorphodiversity on the southeastern side of the valley, corresponding to landforms that are low in variation (mainly water- and glacier-related), with respect to the prevailing gneiss slope (mainly gravity-, glacial-, crinival-, and water-related). In this sense, medium to high geomorphodiversity values are associated with the highest elevation areas of the northwestern slope and the related hanging glacial basin.

Based on the results, the Buscagna stream catchment was then selected to perform a more in-detail analysis, applying the *IC*.

4.2 | Connectivity index maps

The *IC* maps of the Buscagna stream catchment area (Figure 5) differ depending on whether the outlet (Figure 5a), the highest-order stream (Figure 5b), or the lower-order streams (Figure 5c) are selected as a target of the analysis.

In the Buscagna catchment, using the outlet as a target (Figure 5a), the differentiation among the two sides of the valley is clearly visible:

1. Low *IC* values characterize the calcschist slope (sectors E and C). Herein, a structural controlled hydrographic pattern is mainly constituted by V-shaped valleys, trenches, and fractures that interrupt a wide rocky surface shaped by ancient glaciers (C in Figure 5a).
2. High *IC* values characterize the high-relief gneiss slope, especially for debris flow and snow avalanche channels (B1 and B2), re-elaborating glacial and slope debris. These higher *IC* conditions are interrupted for glacial hollows (A1, A2, and A3 in Figure 5a), acting as sediment stores, and for glacial derived scarps, provoking a sudden change in longitudinal connectivity (Bosson et al., 2015; Cavalli, Heckmann, et al., 2019; Messenzehl et al., 2014).

Considering the *IC* calculation based on the highest-order stream (Figure 5b) and the lower-order channels (Figure 5c) as targets of analysis, it is evident that, especially in the latter case, the hydrographic network role on sediment connectivity is even more enhanced and a specific focus should be paid on lateral connectivity. It can be easily observed in Figure 5a how the glacial tributary basins progressively lose differentiation, moving from slopes characterized by high connectivity to the bottom of the basin (A), characterized by low *IC* values, where sediment deposition can be observed.

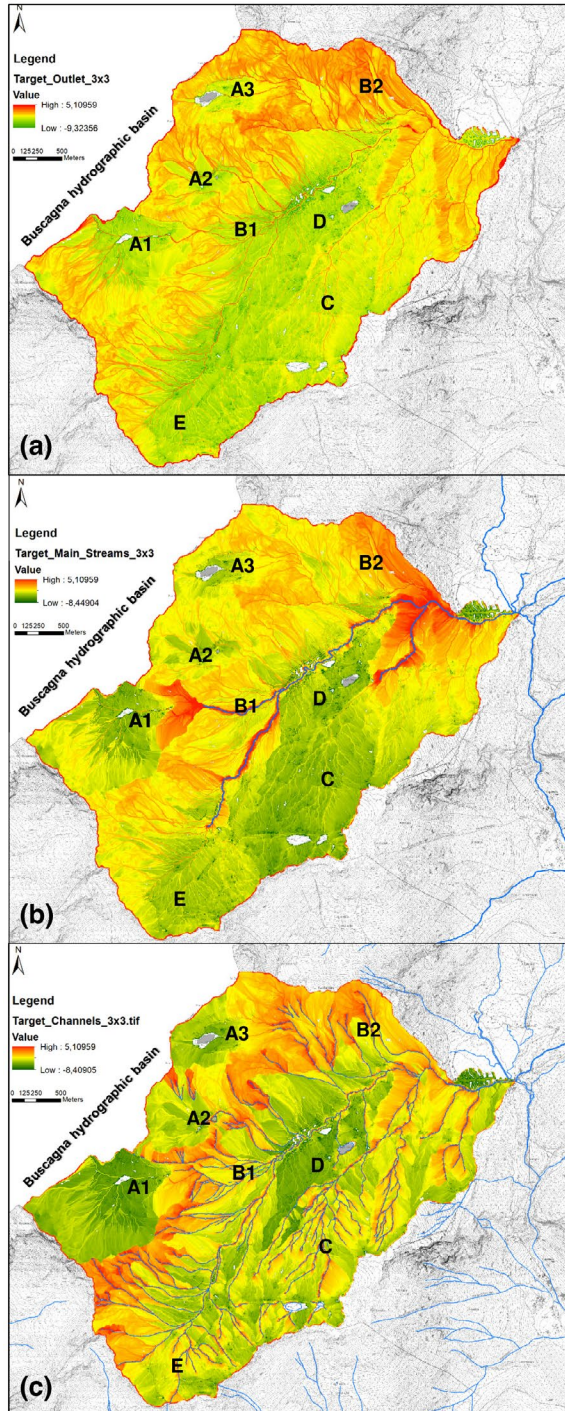


FIGURE 5 IC map for the Buscagna stream catchment using: (a) the outlet; (b) the main streams; and (c) the channels as a target of the analysis

5 | DISCUSSION

The VDNP is a protected area with significant variability in terms of lithology influencing the presence of different relief features, as already highlighted in general for mountain regions (e.g., Bollati et al., 2016; Brocx & Semeniuk, 2007; Zwoliński, 2009) from the regional to the local scale (Gordon, 2018). The *IFrm* and the *IGmf* characterizing the VDNP show a strong correlation depending on the fact that the greater is the number of elements in a cell (*IFrm*), the higher is the possibility they are related to different genetic processes (*IGmf*). In this framework, the *IGmf* could be considered a more conservative index, allowing stronger discrimination among the subareas of a region, a potential that could be interesting for the management and enhancement of protected areas.

Furthermore, in the Buscagna hydrographic basin, selected for an in-depth analysis in relation to the lithological differentiation between slopes, *IGmf* shows medium to high values for the highest elevation areas of the northwestern slope (northern slope) and the related hanging glacial basin. Therein, glacial, crionival, gravity- and water-related landforms, as well as a greater diversification in the lithology, and local structural patterns represent the crucial distinguishing factor. Within a single category of landforms (e.g., glacial, or water- or gravity-related), also the age pattern, the erosion/accumulation distribution and/or the degree of activity of processes could be variable. These factors have not yet been tested in the geomorphodiversity indexing procedure. This will be possible if the geomorphological map database contains all the information, (Gustavsson, Seijmonsbergen, & Kolstrup, 2008), allowing features to be aggregated based on different fields (e.g., *erosion_deposition_type*; *activity_type*), besides using the *landform_type* field (Figure 2).

The role of geomorphological mapping at multi-catchment scale is thus demonstrated to be crucial: as input data (i.e., direct method as *IFrm*, *IGmf*) or, at least, used as comparative data following a morphometry-based indexing procedure (i.e., indirect method; Melelli et al., 2017). In the latter case, Melelli et al. (2017) used a geomorphological map as necessary data to validate their model.

Considering the proportion between the categories of low, medium, and high *IFrm* and *IGmf* values, for a geomorphological similar area of comparable width (285 km²), Hjort and Luoto (2010) found a different range of values, indicating how slightly different methods in geodiversity analyses could affect the final result, and how mountain regions also differ according to local features (Gordon, 2018). Hence the comparison between different regions according to extrinsic geodiversity (sensu Bollati et al., 2016; Panizza, 2009), through quantitative methodologies (i.e., indexing), is far from straightforward.

From the perspective of geoheritage analyses (Zwoliński et al., 2018), *IFrm* and *IGmf* could have different potential applications. *IFrm* provides information on the spatial scale of landforms to be observed in the cell since the greater is the landform mapped in a cell, the lower is the number of landforms that can occupy the cell itself. Anyway, the repetition in terms of categories of landforms and processes may be an issue. In contrast, *IGmf* provides data on variability in processes affecting each cell and could be extremely useful for detecting, with a stronger selection, areas characterized by different processes, in a geotouristic or educational perspective.

The relationship between sediment connectivity patterns and geomorphological features has been well addressed by Messenzehl et al. (2014), who also underlined the importance of geomorphological fieldwork to check the data retrieved using automatic and semi-automatic indexing procedures. Sediment connectivity patterns, then, could have a further relationship with geomorphodiversity, a connection hitherto not yet investigated in detail, and also with the fragmentation of geomorphological elements in the landscape. A significant limit for quantitative comparison of the three indexes (*IFrm*, *IGmf*, and *IC*) is related to the different cell sizes adopted for their computation. If for the *IGmf* and *IFrm* the cell size was chosen as the average dimension of the objects to be considered in the analysis and was of the order of hundreds of meters, for the *IC* computation, measuring a continuum property in the space, the higher is the DTM resolution, the higher is the accuracy of the result since the surface roughness and sediment flow path can be better characterized (Cavalli et al., 2013). It should be also stressed that both indexes are sensitive to resolution (see Figure 2). Similarly, it has been demonstrated that the *IC* is also strongly sensitive to resolution (Brardinoni, Cavalli, Heckmann, Liébault, & Rimböck, 2015; Cantreul,

Biielders, Calsamiglia, & Degré, 2018; Zanandrea, Michel, Kobiyama, & Cardozo, 2019). These studies showed a systematic decrease in IC values with increasing resolution, mainly due to the longer flow direction paths and to higher slope values computed for finer resolutions. The sensitivity to resolution of these indexes may become a critical issue when comparing results using different cell sizes in the case of *IFrm* and *IGmf*, and using DTMs of different resolutions in the case of *IC*. However, a comparison between *IC*, *IFrm*, and *IGmf* thematic maps can be addressed using both semi-quantitative and qualitative approaches.

As anticipated, within the VDNP, the Buscagna stream catchment was selected for the *IC* analysis due to the evident differentiation on the sides of the valley in terms of *IGmf*.

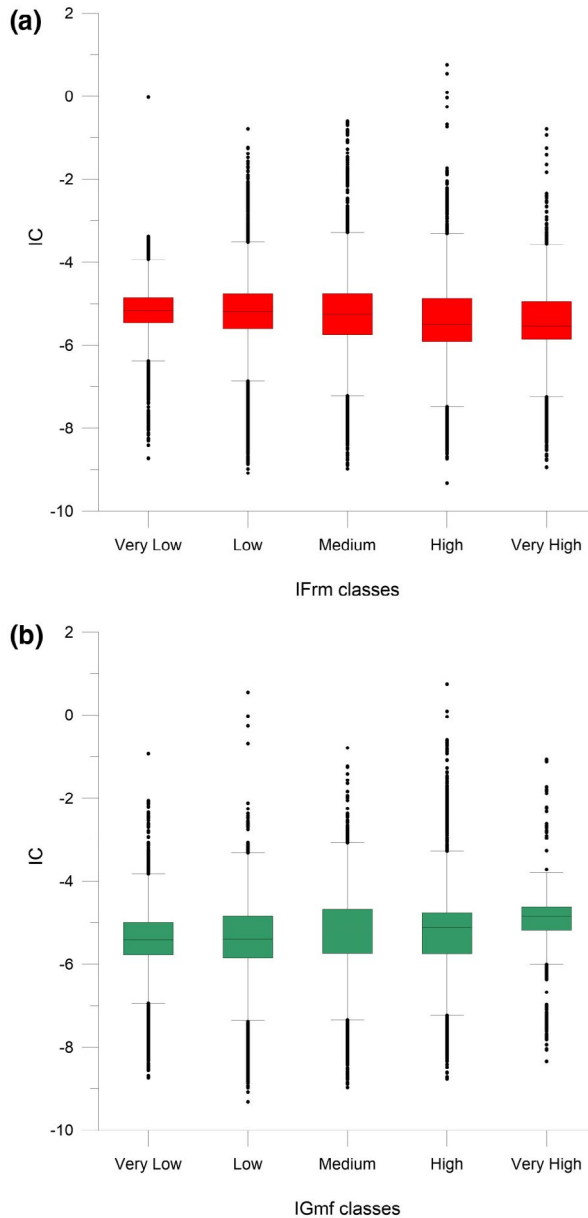


FIGURE 6 Box plots created by transforming the 500 × 500 m grid of the *IFrm* and *IGmf* into a 5 × 5 m grid used for *IC* computation, and showing the relations between *IC* values and *IFrm* and *IGmf* classes

Figure 6 presents box plots showing the relationships between *IC* computed with reference to the outlet (Figure 5a), where the differentiation between the two sides of the valley is clearly visible, and the *IFrm* and *IGmf* classes. The aim is to analyze if a relationship does exist between *IC* values and the other two indexes, or if their relations can be only explained in terms of their spatial structure and the role of the landforms.

The box plots were created by resampling *IFrm* and *IGmf* maps resolution (i.e., 500 × 500 m) to the resolution of *IC* (i.e., 5 × 5 m), in order to allow the direct comparison between *IC* (with respect to the outlet) values and the classes of *IFrm* and *IGmf*. The highest resolution computation was chosen to avoid losing the detailed information on sediment connectivity. It is worth stressing that the main limitation of this approach is related to the possible redundancy of *IFrm* or *IGmf* values when compared to *IC* values. However, the analysis provides interesting outcomes: concerning the *IFrm*–*IC* outlet relation, the *IC* median value shows a decreasing trend with increasing *IFrm* class (Figure 6a), whereas the *IC* median value shows a different trend featuring an increase with increasing *IGmf* class (Figure 6b). The latter relation represents a slight increase in *IC* with increasing geomorphodiversity. We provide a possible explanation for these trends. The increase in the fragmentation of elements in the landscape leads to a decrease in sediment connectivity due to the general increase of the complexity of the system; the higher is the diversity of elements, the lower is the sediment connectivity. The trend changes when the typology of landforms is considered in the *IGmf* computation. This seems also to reflect the good agreement in the spatial pattern between *IGmf* and *IC* (outlet) maps (Figures 4b and 5a). This analysis also highlights that, despite the existing correlation between *IFrm* and *IGmf*, the information provided by the indexes is quite different in relation to their spatial patterns and other landscape parameters as, in this case, sediment connectivity.

Although the box plots already provide some information on the possible interdependence between the parameters, an in-depth examination of their mutual relationships requires a deep knowledge of the area and the assessment of the geomorphological features of the area using an interpretative approach based on *geomorphoconnectivity sectors* (sensu Messenzehl et al., 2014).

As already shown in other case studies concerning the relation between geomorphic processes and sediment connectivity in analogous mountain environments (Cavalli, Heckmann, et al., 2019; Messenzehl et al., 2014), here at least five typologies of *geomorphoconnectivity sectors* could be identified:

- *Hanging glacial basins and connection with valley-bottom* (A1, A2, A3). The glacier-related hollows act as temporary sediment traps (Bosson et al., 2015). They are characterized by a great quantity of debris of glacial and gravity origin, and are surrounded by talus slope deposits. The frontal moraine, in the Cornera basin (A1), is placed on the upper edge of the glacial step that separates the Cornera basin from the valley bottom. The moraine is undergoing dismantling due to paraglacial-type dynamics (sensu Ballantyne, 2002) feeding the B1 composite cone. Despite the potential disconnection between the hanging basin and the valley bottom due to morphometric reasons, where dismantling processes operate (see the area between A1 and B1), a hot spot of sediment connectivity is recorded.
- *Polygenic cones and relative feeding areas* (B1, B2). These are generated by the combination of different processes related to water, gravity, and snow. Debris flow and snow avalanche channels are an effective means of debris transport (Cavalli et al., 2013). These mass wasting processes can play a contrasting role in sediment connectivity since, on the one hand, they contribute to the transport of rocky and woody debris, favoring lateral connectivity, and on the other hand, they can partially dam channels, inducing a decrease in longitudinal connectivity of the streams they impact on, as occurred close to the Buscagna outlet (Masseroli et al., 2020) during 2018 (B2). Avalanche corridors result, consequently, as high connectivity areas considering only as a target of *IC* computation, the secondary channels (Figure 5b,c).
- *Karst-suitable rocky surfaces shaped by glaciers* (C). The drainage of the debris occurs along small V-shaped valleys, often controlled by the structural pattern. More relevant in this case could be the assessment of vertical connectivity, not addressed by the *IC* applied here.

- *Pleistocene glacial deposits* (D). These areas are characterized by widespread, coarse and thick glacial debris. This debris is stocked as relatively high moraines to which the hydrographic network has to adapt, for example changing fluvial pattern just upstream.
- *Karst-suitable block fields* (E). In the head of the valley, marble outcrops have been completely dissected by crioclastism in coarse blocks, between which fine matrix is often absent. The rocks are karst-susceptible, and in this case the connectivity features described for C and D may combine.

Considering the geomorphodiversity and sediment connectivity relationship at the hydrographic basin scale, the *IGmf* map and the *IC-outlet* related map show analogous different patterns along the two slopes of the Buscagna valley (Figures 4b and 5a). The southern slope is characterized by low to medium *IGmf* and *IC-outlet* related values. Considering the *IFrm* and the *IC* maps (Figures 4a and 5), the relationship between *IFrm* and *IC* values seems to be less relevant. Since the *IC* is based on up- and downslope gradient, and on the surface roughness as weighting factor, the evident difference in modeling on the two sides of the valley greatly affects *IC* calculation. In the catchment analyzed, glacial processes turn out to be the main geomorphological controlling factor, at the catchment scale, inhibiting sediment connectivity by favoring sediment storage where: (i) glacial erosion produces gently sloping surfaces (less than 25°) on calcschist (C), (ii) glacial hollows retain sediment on gneiss slope (A1, A2, A3); and (iii) where ancient glacial deposits interrupt valley bottom inducing sedimentation and peatbog formation upstream (D). In contrast, gravity-, snow-, and water-related processes, very active on the northern slope, favor sediment delivery (B1, B2).

According to these descriptive considerations, moving to a finer spatial scale, one could state that the higher are the *IFrm* and *IGmf* values, the more disturbed the sediment connectivity pattern could be. The frequent spatial variation between geomorphic elements can affect the continuity of sediment delivery through the landscape system (i.e., *structural connectivity*), inducing abrupt interruptions. This is also true for geomorphic processes (i.e., *functional connectivity*). In any case polyline-type elements, like debris flow or snow avalanche channels, represent prevalent sediment delivery paths favoring lateral connectivity between different system sectors.

Taking box-plot outcomes, resulting from using *IFrm* and *IGmf* classes, and geomorphoconnectivity sector interpretations together, it emerges that:

1. the northern slope is more diverse, with higher *IGmf* (mainly medium; Figure 4b), and is characterized also by high *IC* (Figure 5), favored mainly by gravity- and water-related processes;
2. the southern slope is less diverse, with lower *IGmf* (mainly very low; Figure 4b), and is characterized by low *IC*, especially considering the *IC-outlet* (Figure 5a).

Since the *IFrm* index does not consider the type of landforms but only their number, the spatial trend is less clustered within the catchment (Figure 4a), and only through the box plots is it possible to emphasize the inverse relation existing between the fragmentation degree and the sediment connectivity.

The workflow of the analyses is presented in Figure 7. It shows how geomorphological classification and mapping of an area is fundamental at different scales: changing from the regional to the basin spatial scale for the analyses on *IGmf* and *IC-outlet related*, as far as the local scale especially for the analyses on the *IC - secondary streams related*.

Although, as underlined by other authors (e.g., Melelli et al., 2017), a direct method like the one proposed here is limited by the availability of geomorphological maps and the relative subjectivity that is intrinsic to their creation, the approach employed is a semi-objective method that can be extended to other contexts. Due to the aim of the method applied here, the interpretation of the landforms genesis is required in order to compare the geomorphology-related indexes (*IFrm* and *IGmf*) with a morphometric index (*IC*). Moreover, a cross-check involving the comparison of indexes derived from the geomorphological map (*IFrm* and *IGmf*) with an objective index like the *IC*, which is quite well related to geomorphology, could partly address the subjectivity issue.

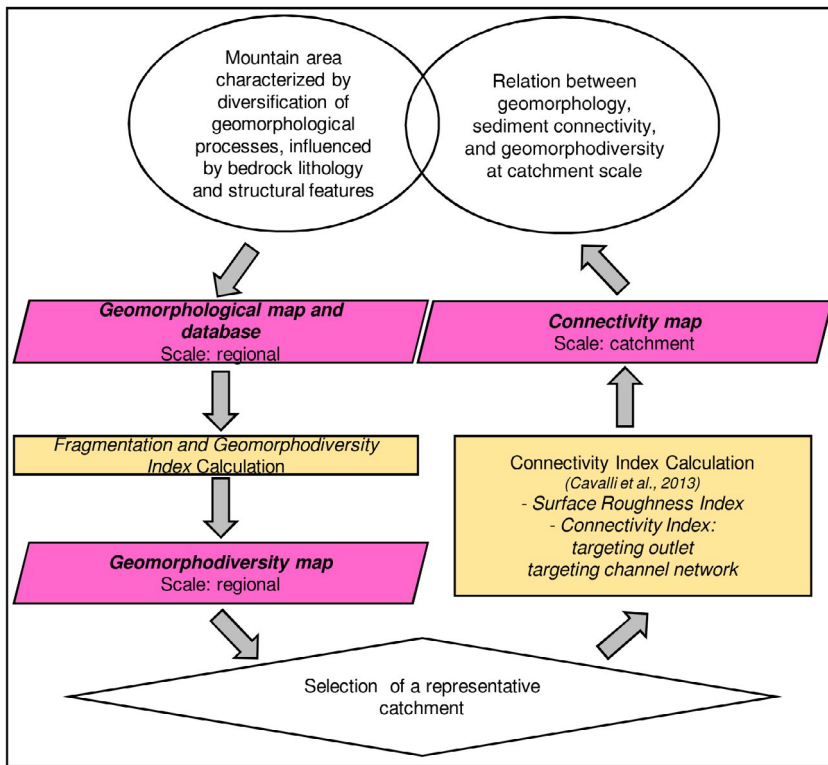


FIGURE 7 Workflow of the geomorphodiversity and sediment connectivity comparison analysis

The fast running of these GIS procedures potentially allows the thematic maps to be frequently updated, particularly useful when landscape modifications occur. As highlighted by Zwoliński (2009), mountain environments, highly sensitive to climate change (Beniston, 2003), are characterized by a dynamic geodiversity: each modification to the digital geomorphological map and the generation of new DTMs in areas of altered morphometry could be followed by a quick rerunning of this entire procedure to create updated *IFrm* and *IGmf* and *IC* maps.

Finally, the production of simple tools applicable autonomously by stakeholders and territorial managers represents an additional impact on society in the view of enhancing and protecting the territory's natural heritage.

6 | CONCLUSIONS

In the present research, the *IGmf* was expected to provide information at VDNP scale (500 × 500 m cell size) and, according to the results of the *IGmf*, the *IC* (computed based on a 5 × 5 m DTM) was derived in the Buscagna small mountain catchment, where the relationship between sediment connectivity, geomorphic processes and geomorphodiversity could be relevant due to the particular lithological dichotomy characterizing its slope. Moreover, the area has been considered a test-site for different scientific purposes linked with geomorphology (e.g., Masseroli et al., 2020).

The *IGmf* turned out to be more conservative than the *IFrm* and more management-oriented for protected areas, like the VDNP. The *IC* is confirmed as very suitable for small mountain catchments characterized by a local diversification of geomorphic processes and a complex topography. Using the outlet as a target or the highest-order stream or, even more, the lower-order channels, the *IC* provides a different detail on sediment delivery

processes. Hence, for this reason, the coupling of an IC map with a geomorphological map and a IGmf map, a quite novel approach, is necessary using the highest-order stream, and shown to be useful in the case of lower-order channels.

In general, these research findings stress the need for geomorphological interpretation in support of semi-quantitative GIS analysis for an in-depth analysis of the mutual relationships between geomorphodiversity and sediment connectivity. Geomorphoconnectivity sectors provide an approach integrating semi-quantitative GIS-based analysis and geomorphological interpretation that proved to be useful in investigating landscape properties such as geomorphodiversity and sediment connectivity. From a more practical point of view, the combination of indexes proposed in this work is intended for a first rapid mapping of these properties in a catchment and could provide a useful tool for a first insight into the landscape under investigation.

The pronounced diversity between slopes in terms of geomorphic dynamics could also influence soil and vegetation patterns, as investigated for this region in detail by Masseroli et al. (2020). Considering the effects of geomorphic processes and sediment connectivity on these other components of the ecosystem (Cavalli, Vericat, et al., 2019; Savi et al., 2013), a holistic approach (Seijmonsbergen et al., 2019) is recommended in future research, especially in protected areas such as the one investigated in the framework of this research.

ACKNOWLEDGMENTS

The authors are grateful to Dr. Maria Paleari, Dr. Anna Masseroli, Prof. M. Pelfini and the Ente Gestione Aree Protette dell'Ossola for the factive and supporting collaboration to the research.

CONFLICT OF INTEREST

The authors do not have any conflict of interest.

DATA AVAILABILITY STATEMENT

The data that support the findings of this study are available from the corresponding author upon reasonable request.

ORCID

Irene Maria Bollati  <https://orcid.org/0000-0002-9195-8008>

Marco Cavalli  <https://orcid.org/0000-0001-5937-454X>

REFERENCES

- Ballantyne, C. K. (2002). Paraglacial geomorphology. *Quaternary Science Review*, 21(18–19), 1935–2017. [https://doi.org/10.1016/S0277-3791\(02\)00005-7](https://doi.org/10.1016/S0277-3791(02)00005-7)
- Baroni, C., Gentili, R., & Armiraglio, S. (2013). Vegetation analysis on composite debris cones. In M. Stoffel, F. Rudolf-Miklau, & M. Schneuwly-Bollsweiler (Eds.), *Dating torrential processes on fans and cones* (pp. 187–201). Dordrecht, the Netherlands: Springer.
- Beniston, M. (2003). Climatic change in mountain regions: A review of possible impacts. In H. F. Diaz (Ed.), *Climate variability and change in high elevation regions: Past, present & future* (pp. 5–31). Dordrecht, the Netherlands: Springer.
- Bigioggero, B., Colombo, A., Cavallo, A., Aldighieri, B., & Tunesi, A. (2007). *Geological-structural sketch-map of the Ossola-Simplon area*. Snam Rete Gas Ed., 1 map; 1: 50,000 scale. Firenze, Italy: Litografia Artistica Cartografica.
- Boeckli, L., Brenning, A., Gruber, S., & Noetzli, J. (2012). Permafrost distribution in the European Alps: Calculation and evaluation of an index map and summary statistics. *The Cryosphere*, 6(4), 807–820. <https://doi.org/10.5167/uzh-67122>
- Bollati, I. M., Cerrato, R., Crosa Lenz, B., Vezzola, L., Giaccone, E., Viani, C., ... Guglielmin, M. (2018). Geomorphological map of the Val Viola Pass (Italy-Switzerland). *Geografia Fisica e Dinamica Quaternaria*, 41(2), 105–114. <https://doi.org/10.4461/GFDQ.2018.41.16>
- Bollati, I. M., Crosa Lenz, B., Golzio, A., & Masseroli, A. (2018). Tree rings as ecological indicator of geomorphic activity in geoheritage studies. *Ecological Indicators*, 93, 899–916. <https://doi.org/10.1016/j.ecolind.2018.05.053>
- Bollati, I., Fossati, M., Zanoletti, E., Zucali, M., Magagna, A., & Pelfini, M. (2016). A methodological proposal for the assessment of cliffs equipped for climbing as a component of geoheritage and tools for Earth Science education: The case

- of the Verbano-Cusio-Ossola (Western Italian Alps). In E. Skourtsos & G. Lister (Eds.), *General contributions, Journal of the Virtual Explorer* (electronic edition; Vol. 49, No. 1, pp. 1–23). Conder, Australia: The Virtual Explorer Pty. Ltd.
- Bollati, I. M., Paleari, M., Zanoletti, E., & Pelfini, M. (2017). Indexing geomorphodiversity in the Veglia-Devero Natural Park (Western Italian Alps). In M. Pennetta & I. M. Bollati (Eds.), *Innovative technologies for monitoring past and present geomorphological processes. Proceedings of the VIIth Young Geomorphologists' Day*, Naples, 15–16 June. Naples, Italy: AIGeo - Italian Association of Physical Geography and Geomorphology.
- Borselli, L., Cassi, P., & Torri, D. (2008). Prolegomena to sediment and flow connectivity in the landscape: A GIS and field numerical assessment. *Catena*, 75, 268–277. <https://doi.org/10.1016/j.catena.2008.07.006>
- Bosson, J. B., Deline, P., Bodin, X., Schoeneich, P., Baron, L., Gardent, M., & Lambiel, C. (2015). The influence of ground ice distribution on geomorphic dynamics since the Little Ice Age in proglacial areas of two cirque glacier systems. *Earth Surface Processes and Landforms*, 40(5), 666–680. <https://doi.org/10.1002/esp.3666>
- Brardinoni, F., Cavalli, M., Heckmann, T., Liébault, F., & Rimböck, A. (2015). *Guidelines for assessing sediment dynamics in alpine basins and channel reaches* (Final Report of the SedAlp Project, Work Package 4). Vienna, Austria.
- Brierley, G., Fryirs, K., & Jain, V. (2006). Landscape connectivity. The geographic basis of geomorphic applications. *Area*, 38(2), 165–174. <https://doi.org/10.1111/j.1475-4762.2006.00671.x>
- Brocx, M., & Semeniuk, V. (2007). Geoheritage and geoconservation: History, definition, scope and scale. *Journal of the Royal Society of Western Australia*, 90(2), 53–87. <http://researchrepository.murdoch.edu.au/id/eprint/10140>
- Buter, A., Spitzer, A., Comiti, F., & Heckmann, T. (2020). Geomorphology of the Sulden River basin (Italian Alps) with a focus on sediment connectivity. *Journal of Maps*, 16(2), 890–901. <https://doi.org/10.1080/17445647.2020.1841036>
- Campobasso, C., Carton, A., Chelli, A., D'Orefice, M., Dramis, F., Graciotti, R., ... Pellegrini, L. (2018). Carta Geomorfologica d'Italia alla scala 1:50.000. Aggiornamento ed integrazioni delle linee guida della Carta Geomorfologica d'Italia alla scala 1:50.000 (Fascicolo I). In *Quaderni del Servizio Geologico Nazionale, Ser. III, 13* (96 pp.). Rome, Italy: Istituto Poligrafico e Zecca dello Stato.
- Cantreul, V., Bièlders, C., Calsamiglia, A., & Degré, A. (2018). How pixel size affects a sediment connectivity index in central Belgium. *Earth Surface Processes and Landforms*, 43, 884–893. <https://doi.org/10.1002/esp.4295>
- Carcavilla, L., López-Martínez, J., & Durán, J. J. (2007). *Patrimonio geológico y geodiversidad: Investigación, conservación, gestión y relación con los espacios naturales protegidos* (Serie Cuadernos del Museo Geominero, 7). Madrid, Spain: Instituto Geológico y Minero de España.
- Castiglioni, G. B. (1966). Considerazioni su un congresso internazionale di Geomorfologia. *Rivista Geografica Italiana*, 73(4), 476–487.
- Cavalli, M., Heckmann, T., & Marchi, L. (2019). Sediment connectivity in proglacial areas. In T. Heckmann & D. Morche (Eds.), *Geomorphology of proglacial systems* (pp. 271–287). Cham, Switzerland: Springer.
- Cavalli, M., & Marchi, L. (2008). Characterisation of the surface morphology of an alpine alluvial fan using airborne LiDAR. *Natural Hazards and Earth System Sciences*, 8(2), 323–333. <https://doi.org/10.5194/nhess-8-323-2008>
- Cavalli, M., Trevisani, S., Comiti, F., & Marchi, L. (2013). Geomorphometric assessment of spatial sediment connectivity in small Alpine catchments. *Geomorphology*, 188, 31–41. <https://doi.org/10.1016/j.geomorph.2012.05.007>
- Cavalli, M., Vericat, D., & Pereira, P. (2019). Mapping water and sediment connectivity. *Science of the Total Environment*, 673, 763–767. <https://doi.org/10.1016/j.scitotenv.2019.04.071>
- Chandler, B. M. P., Lovell, H., Boston, C. M., Lukas, S., Barr, I. D., Benediktsson, Í. Ö., ... Stroeven, A. P. (2018). Glacial geomorphological mapping: A review of approaches and frameworks for best practice. *Earth-Science Reviews*, 185, 806–846. <https://doi.org/10.1016/j.earscirev.2018.07.015>
- Crema, S., & Cavalli, M. (2018). SedInConnect: A stand-alone, free and open source tool for the assessment of sediment connectivity. *Computer & Geosciences*, 111, 39–45. <https://doi.org/10.1016/j.cageo.2017.10.009>
- Diolaiuti, G., & Smiraglia, C. (2015). *Il nuovo catasto dei ghiacciai italiani* (pp. 134–138). Ev-K2-CNR, Bergamo Publications.
- Dixon, G. (1996). *Geoconservation: An international review and strategy for Tasmania* (Occasional Paper 35). Tasmania, Australia: Parks and Wildlife Service.
- Fryirs, K. A. (2013). (Dis)connectivity in catchment sediment cascades: A fresh look at the sediment delivery problem. *Earth Surface Processes and Landforms*, 38(1), 30–46. <https://doi.org/10.1002/esp.3242>
- Fryirs, K. A., & Brierley, G. J. (2018). What's in a name? A naming convention for geomorphic river types using the River Styles Framework. *PLoS ONE*, 13(9), e0201909. <https://doi.org/10.1371/journal.pone.0201909>
- Fryirs, K. A., Brierley, G. J., Preston, N. J., & Kasai, M. (2007). Buffers, barriers and blankets: The (dis)connectivity of catchment-scale sediment cascades. *Catena*, 70(1), 49–67. <https://doi.org/10.1016/j.catena.2006.07.007>
- Gentizon, C., Baud, M., Holzmann, C., Lambiel, C., Reynard, E., & Schoeneich, P. (2000). GIS and geomorphological mapping as management tools in alpine periglacial areas. *High Mountain Cartography*, 18, 215–228.
- Germain, D., Gavrilă, I. G., Elizbalashvili, M., & Pop, O. T. (2020). Multidisciplinary approach to sediment connectivity between debris-flow channel network and the Dolra River, Mazeri Valley, Southern Caucasus, Georgia. *Geomorphology*, 371, 107455. <https://doi.org/10.1016/j.geomorph.2020.107455>

- Gordon, J. E. (2018). Mountain geodiversity: Characteristics, values and climate change. In A. Antonelli, A. Perrigo, & C. Hoorn (Eds.), *Mountains, climate and biodiversity* (pp. 137–154). Chichester, UK: John Wiley & Sons.
- Gray, M. (2004). *Geodiversity: Valuing and conserving abiotic nature*. Chichester, UK: John Wiley & Sons.
- Gray, M., Gordon, J. E., & Brown, E. J. (2013). Geodiversity and the ecosystem approach: The contribution of geoscience in delivering integrated environmental management. *Proceedings of the Geologists' Association*, 124(4), 659–673. <https://doi.org/10.1016/j.pgeola.2013.01.003>
- Gustavsson, M., Seijmonsbergen, A. C., & Kolstrup, E. (2008). Structure and contents of a new geomorphological GIS database linked to a geomorphological map—With an example from Liden, central Sweden. *Geomorphology*, 95(3–4), 335–349. <https://doi.org/10.1016/j.geomorph.2007.06.014>
- Harvey, A. M. (2001). Coupling between hillslopes and channels in upland fluvial systems: Implications for landscape sensitivity, illustrated from the Howgill Fells, Northwest England. *Catena*, 42(2–4), 225–250. [https://doi.org/10.1016/S0341-8162\(00\)00139-9](https://doi.org/10.1016/S0341-8162(00)00139-9)
- Heckmann, T., Cavalli, M., Cerdan, O., Foerster, S., Javaux, M., Lode, E., ... Brardinoni, F. (2018). Indices of sediment connectivity: Opportunities, challenges and limitations. *Earth-Science Review*, 187, 77–108. [10.1016/j.earscirev.2018.08.004](https://doi.org/10.1016/j.earscirev.2018.08.004)
- Hjort, J., & Luoto, M. (2010). Geodiversity of high-latitude landscapes in northern Finland. *Geomorphology*, 115(1–2), 109–116. <https://doi.org/10.1016/j.geomorph.2009.09.039>
- Hjort, J., & Luoto, M. (2012). Can geodiversity be predicted from space? *Geomorphology*, 153, 74–80. <https://doi.org/10.1016/j.geomorph.2012.02.010>
- Hooke, J. (2003). Coarse sediment connectivity in river channel systems: A conceptual framework and methodology. *Geomorphology*, 56(1–2), 79–94. [https://doi.org/10.1016/S0169-555X\(03\)00047-3](https://doi.org/10.1016/S0169-555X(03)00047-3)
- Masseroli, A., Bollati, I. M., Proverbio, S. S., Pelfini, M., & Trombino, L. (2020). Soils as a useful tool for reconstructing geomorphic dynamics in high mountain environments: The case of the Buscagna stream hydrographic basin (Lepontine Alps). *Geomorphology*, 371, 107442. <https://doi.org/10.1016/j.geomorph.2020.107442>
- Melelli, L., Vergari, F., Liucci, L., & Del Monte, M. (2017). Geomorphodiversity index: Quantifying the diversity of landforms and physical landscape. *Science of the Total Environment*, 584, 701–714. <https://doi.org/10.1016/j.scitotenv.2017.01.101>
- Messenzehl, K., Hoffmann, T., & Dikau, R. (2014). Sediment connectivity in the high-alpine valley of Val Mütschuns, Swiss National Park—Linking geomorphic field mapping with geomorphometric modelling. *Geomorphology*, 221, 215–229. <https://doi.org/10.1016/j.geomorph.2014.05.033>
- Otto, J. C., Schrott, L., Jaboyedoff, M., & Dikau, R. (2009). Quantifying sediment storage in a high alpine valley (Turtmanntal, Switzerland). *Earth Surface Processes and Landforms*, 34(13), 1726–1742. <https://doi.org/10.1002/esp.1856>
- Panizza, M. (2009). The geomorphodiversity of the Dolomites (Italy): A key of geoheritage assessment. *Geoheritage*, 1, 33–42. <https://doi.org/10.1007/s12371-009-0003-z>
- Pellitero, R., Manosso, F. C., & Serrano, E. (2015). Mid-and large-scale geodiversity calculation in fuentes carrionas (NW Spain) and serra do cadeado (Paraná, Brazil): Methodology and application for land management. *Geografiska Annaler: Series A, Physical Geography*, 97(2), 219–235. <https://doi.org/10.1111/geoa.12057>
- Pereira, D. I., Pereira, P., Brilha, J., & Santos, L. (2013). Geodiversity assessment of Paraná State (Brazil): An innovative approach. *Environmental Management*, 52(3), 541–552. <https://doi.org/10.1007/s00267-013-0100-2>
- Rădoane, M., Cristea, I., & Rădoane, N. (2011). Geomorphological mapping. Evolution and trends. *Revista de Geomorfologie*, 13, 19–40. https://doi.org/10.1007/978-3-319-32589-7_18
- Rigamonti, I., & Uggeri, A. (2016). L'evoluzione dell'Alpe Veglia nel quadro delle Alpe Centrali. *Geologia Insubrica*, 2016(1), 69–83.
- Sacco, F. (1930). *Il glacialismo nelle valli Sesia, Strona, Anza e nell'Ossola: memoria*. Rome, Italy: Provveditorato generale dello Stato.
- Savi, S., Schneuwly-Bollschweiler, M., Bommer-Dennis, B., Stoffel, M., & Schlunegger, F. (2013). Geomorphic coupling between hillslopes and channels in the Swiss Alps. *Earth Surface Processes and Landforms*, 38(9), 959–969. <https://doi.org/10.1002/esp.3342>
- Seijmonsbergen, A. C., Van den Ancker, J. A. M., Jungerius, P. D., & Norder, S. J. (2019). Can geodiversity help to save the soil archives? In J. J. Van Mourik & J. M. Van Der Meer (Eds.), *Reading the soil archives – Unravelling the geoecological code of paleosols and sediment cores. Developments in Quaternary Science* (Vol. 18, pp. 275–298). Amsterdam, Netherlands: Elsevier. <https://doi.org/10.1016/B978-0-444-64108-3.00008-2>
- Singh, M., & Sinha, R. (2020). Distribution, diversity, and geomorphic evolution of floodplain wetlands and wetland complexes in the Ganga plains of north Bihar, India. *Geomorphology*, 351, 106960. <https://doi.org/10.1016/j.geomorph.2019.106960>
- Singh, M., Sinha, R., & Tandon, S. K. (2021). Geomorphic connectivity and its application for understanding landscape complexities: A focus on the hydro-geomorphic systems of India. *Earth Surface Processes and Landforms*, 46(1), 110–130. <https://doi.org/10.1002/esp.4945>

- Steck, A. (2008). Tectonics of the Simplon massif and Lepontine gneiss dome: Deformation structures due to collision between the underthrusting European plate and the Adriatic indenter. *Swiss Journal of Geosciences*, 101(2), 515–546. <https://doi.org/10.1007/s00015-008-1283-z>
- Theler, D., Reynard, E., Lambiel, C., & Bardou, E. (2010). The contribution of geomorphological mapping to sediment transfer evaluation in small alpine catchments. *Geomorphology*, 124(3–4), 113–123. <https://doi.org/10.1016/j.geomorph.2010.03.006>
- Verstappen, H. T. (2011). Old and new trends in geomorphological and landform mapping. *Developments in Earth Surface Processes*, 15, 13–38. <https://doi.org/10.1016/B978-0-444-53446-0.00002-1>
- Wainwright, J., Turnbull, L., Ibrahim, T. G., Lexartza-Artza, I., Thornton, S. F., & Brazier, R. E. (2011). Linking environmental régimes, space and time: Interpretations of structural and functional connectivity. *Geomorphology*, 126, 387–404. <https://doi.org/10.1016/j.geomorph.2010.07.027>
- Washington, H. (2018). The intrinsic value of geodiversity. *The Ecological Citizen*, 1(2), 2018.
- Wheaton, J. M., Fryirs, K. A., Brierley, G., Bangen, S. G., Bouwes, N., & O'Brien, G. (2015). Geomorphic mapping and taxonomy of fluvial landforms. *Geomorphology*, 248, 273–295. <https://doi.org/10.1016/j.geomorph.2015.07>
- Zanandrea, F., Michel, G. P., Kobiyama, M., & Cardozo, G. L. (2019). Evaluation of different DTMs in sediment connectivity determination in the Mascarada River Watershed, southern Brazil. *Geomorphology*, 332, 80–87. <https://doi.org/10.1016/j.geomorph.2019.02.005>
- Zwoliński, Z. (2009). The routine of landform geodiversity map design for the Polish Carpathian Mts. *Landform Analysis*, 11, 77–85.
- Zwoliński, Z., Najwer, A., & Giardino, M. (2018). Methods for assessing geodiversity. In E. Reynard & J. Brilha (Eds.), *Geoheritage: Assessment, protection, and management* (pp. 27–52). Amsterdam, the Netherlands: Elsevier. <https://doi.org/10.1016/B978-0-12-809531-7.00002-2>

SUPPORTING INFORMATION

Additional Supporting Information may be found online in the Supporting Information section.



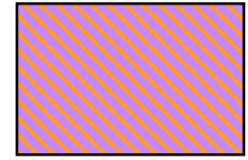

How to cite this article: Bollati, I. M., & Cavalli, M. (2021). Unraveling the relationship between geomorphodiversity and sediment connectivity in a small alpine catchment. *Transactions in GIS*, 00, 1–20. <https://doi.org/10.1111/tgis.12793>

SUPPLEMENTARY FILE

VEGLIA DEVERO NATURAL PARK GEOMORPHOLOGICAL MAP Input data for IFrm and IGmf calculation

LITOLOGY

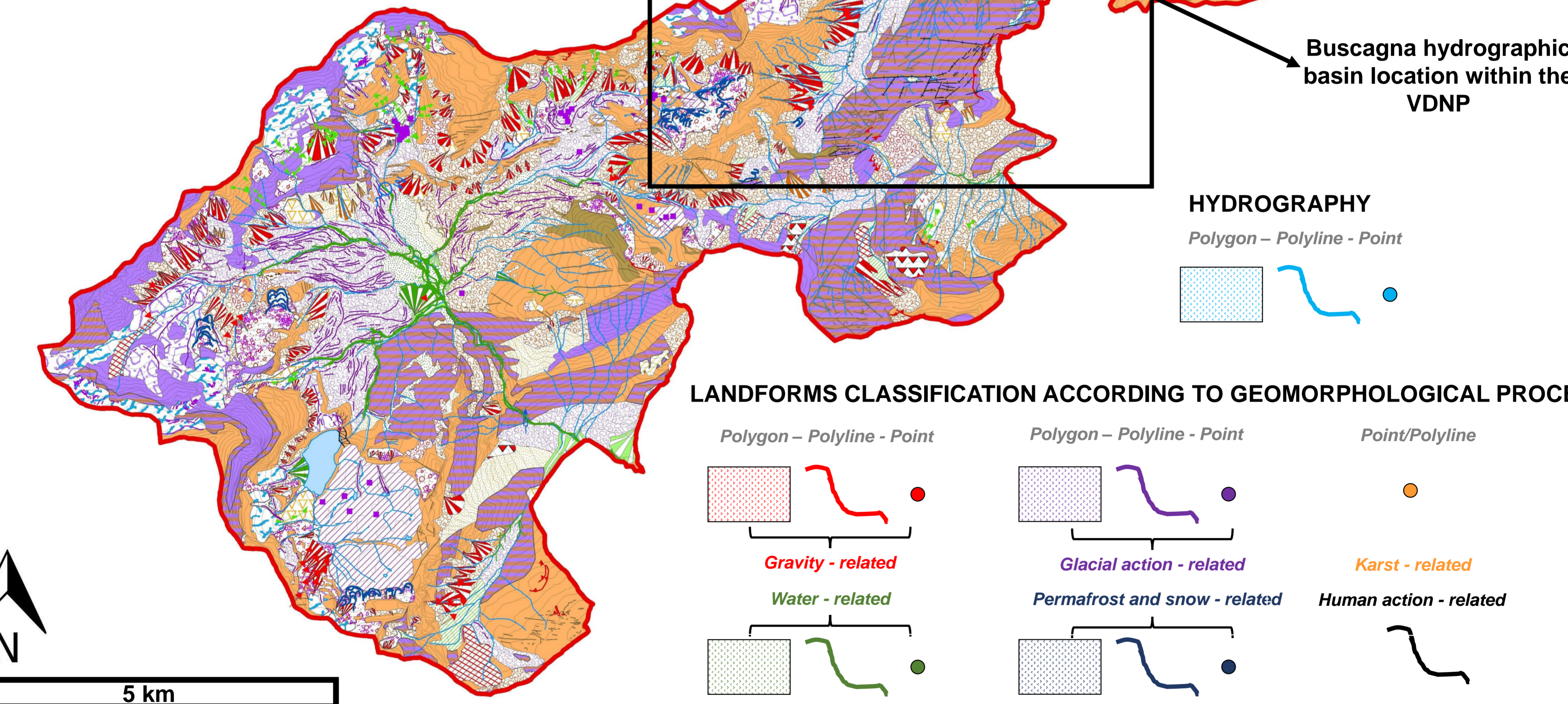
Polygon

-  Massive metamorphic and intrusive rocks (e.g., amphibolites, granite, ortogneiss)
-  Foliated metamorphic rocks (e.g. micaschist, phyllades, serpentinites)
-  Foliated and soluble metamorphic rocks (e.g. calcschist)
-  Soluble rocks (e.g. limestone, gypsum, anhydrite)

STRUCTURES

Polyline

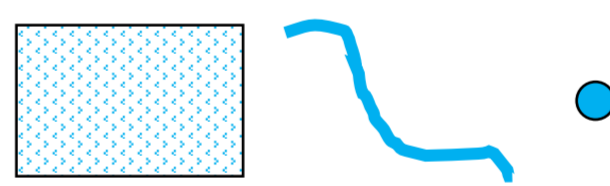
Faults/fractures



Buscagna hydrographic basin location within the VDNP

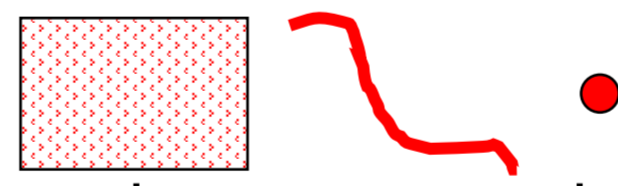
HYDROGRAPHY

Polygon - Polyline - Point



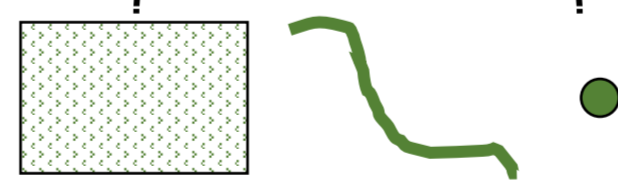
LANDFORMS CLASSIFICATION ACCORDING TO GEOMORPHOLOGICAL PROCESS

Polygon - Polyline - Point

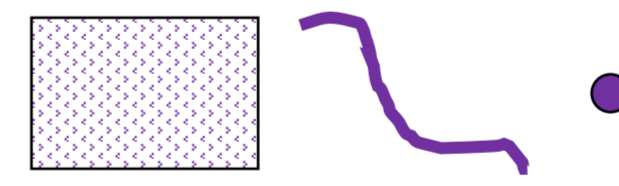


Gravity - related

Water - related

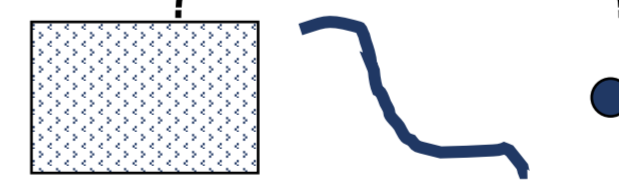


Polygon - Polyline - Point

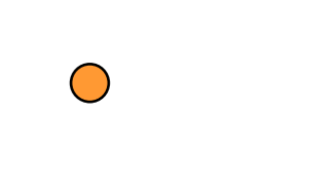


Glacial action - related

Permafrost and snow - related



Point/Polyline



Karst - related

Human action - related

